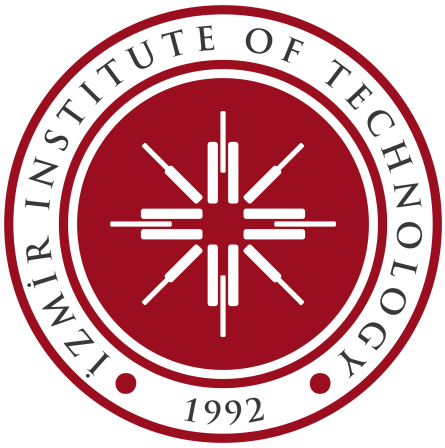

İzmir Institute of Technology

Introduction to Robot Technology

ME460

Project #3

Quasi-Static Force Analysis of Serial RRP Manipulator

Mert Emrem - 250203015

Mechanical Engineering

Summer 2021

Contents

Introduction

The manipulator architecture is identical to the ones used in project #1 and #2 [1, 2], namely, *spherical arm* (RRP), with dimensional parameter d_1, and joint parameters θ_1, θ_2, s_3 as shown in figure 1.1 below.

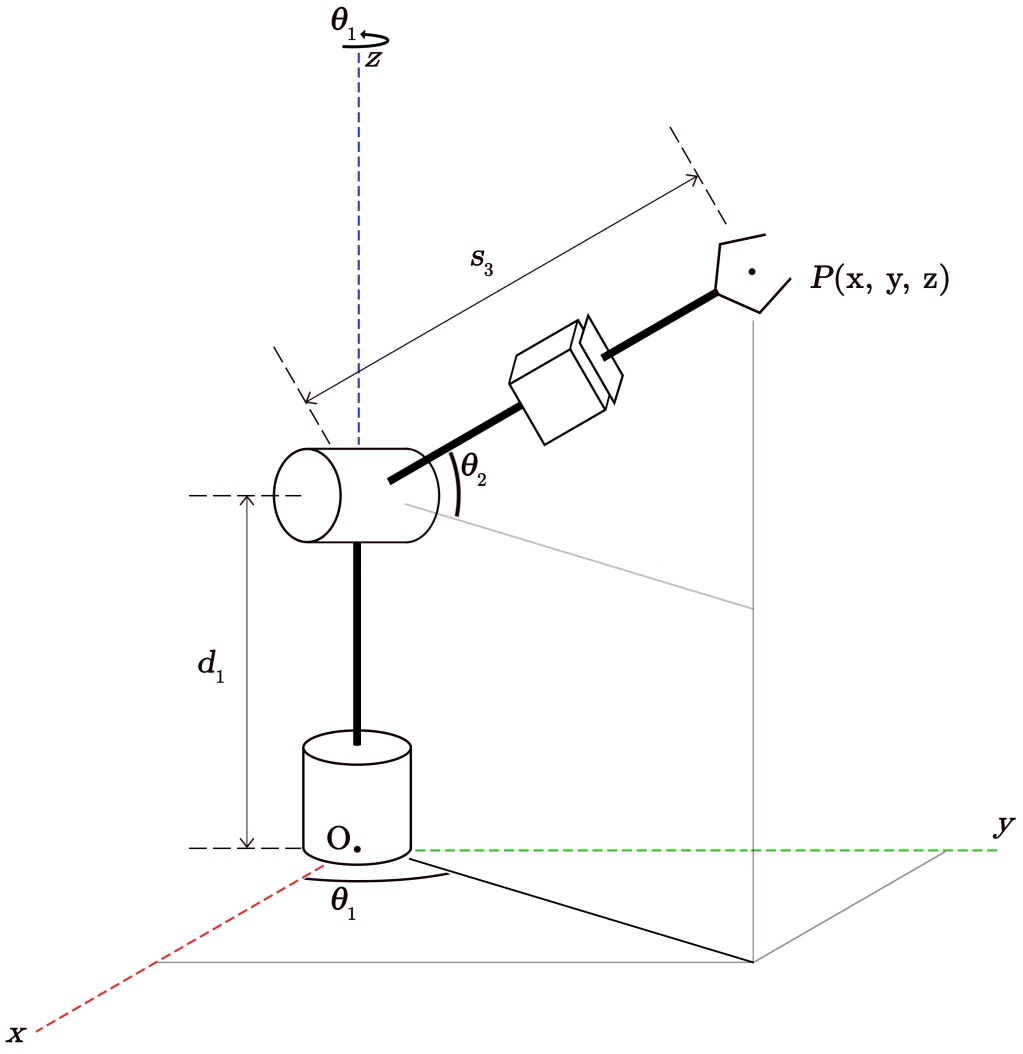

Figure 1.1: Kinematic diagram of the RRP manipulator [1].

Starting dimensions and constraints are as follows:

from projects #1 and #2:

$$d_1 = 125 \text{ mm} \qquad s_{3,\,\max} = 125 \text{ mm} \qquad (s_{3,\min} = 0 \text{ mm})$$
$$v_{\max} = 16 \text{ mm/s}^2 \qquad a_{\max} = 37.5 \text{ mm/s}^2$$

Student number: $\underline{25}0203015$

$$F_x : 5 + 10 = 15 \text{ N} \qquad F_y : (5 - 15) \times 2 = -20 \text{ N} \qquad F_z : \underline{25} - 10 = 15 \text{ N}$$
$$m_1 : (5 + 10)/2 = 7.5 \text{ kg} \qquad m_2 : (5 + 5)/2 = 5 \text{ kg} \qquad m_3 : (5 + 1)/2 = 3 \text{ kg}$$

Gravitational acceleration is assumed constant at: $\vec{g} = -9.81\hat{k}$ mm/s^2

Home position is defined by $\theta_1 = 0$, $\theta_2 = 0$, and $s_3 = 125$ mm.

Reference frame is at the base point, O (also the first revolute joint, R_1), with z axis coinciding with the rotation axis of R_1, as shown in fig. 1.1.

All bodies are assumed to be rigid, and the joints are assumed to have no clearances.

In the first two projects, forward and inverse kinematics relations of the manipulator were derived, and were applied on an $x - y - z$ composite trajectory, throughout which joint space parameters were derived. This part of the project focuses on the force and gravitational effects on the manipulator, and the actuator torques/forces required to counter them. Quasi-static force analysis methods are used, and the reaction joint torques/forces are computed with regards to gravitational load, and separately, the external force F applied at the end-effector. Dynamic analysis of the manipulator falls outside the purview of the given task, and therefore inertial and Coriolis effects are disregarded. General dynamic equation of a manipulator is as follows.

$$\hat{M}(\bar{q})\ddot{\bar{q}} + \hat{B}(\bar{q}, \dot{\bar{q}}) + \bar{G}(\bar{q}) = \bar{\tau}_a + \bar{\tau}_e + \bar{\tau}_d \tag{1.1}$$

1.1 Modeling Approach

In modeling the manipulator, for which not all link lengths are specified, two options arise: One model shown in fig 1.2a, where $s_{3,\min} = a_2$, which does a good job of representing real-life telescopic RRP manipulators is sufficient for the trajectory chosen, or the model in which the link a_2 is ditched completely and the prismatic joint P_1 is coincident with R_2, which is basically a Stanford arm sans the offset between R_2 and P_1, as shown in fig 1.2b. Note that the former necessitates an additional link and therefore mass.

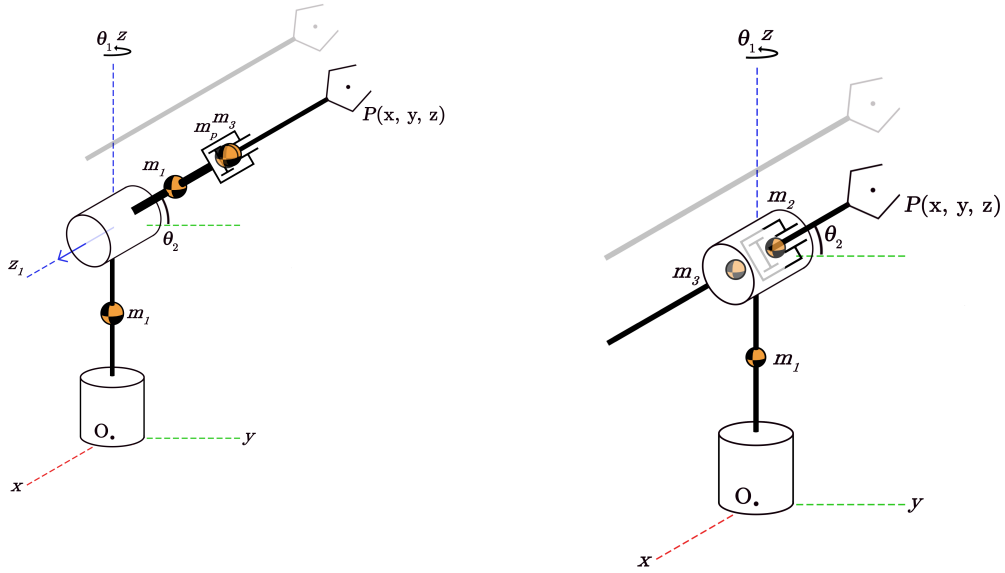

(a) Approach A[a]

[a]Upper m_1 is supposed to read m_2.

(b) Approach B

Figure 1.2: The alternative methods considered while modeling the manipulator.

All centers of mass are at the midpoints of their respective links.

1.2 Position and Velocity-Level Kinematics

Forward kinematics equations developed for the manipulator are:

$$P_x = s_3 \cos\theta_2 \cos\theta_1 \tag{1.2}$$

$$P_y = s_3 \cos\theta_2 \sin\theta_1 \tag{1.3}$$

$$P_z = d_1 + s_3 \sin\theta_2 \tag{1.4}$$

...Tip point P being a function of θ_1, θ_2, and s_3.

Inverse kinematics equations developed for the manipulator are:

$$\theta_1 = \arctan2(P_x, P_y) \tag{1.5}$$

$$\theta_2 = \arctan2(r, l) \tag{1.6}$$

$$s_3 = |(\sigma)\sqrt{r^2 + l^2}| \tag{1.7}$$

where $l = z - d_1$ and $r = |(\sigma)\sqrt{x^2 + y^2}|$, and σ represents sign ambiguity arising from taking the square root of the equation. Values s_3 and r are absolute lengths, and therefore the negative values can be discarded. From 1.7, s_3 has a double solution for $-l$ and $+l$,

From eqs. 1.5 and 1.6, a double solution is apparent, which is for any P,
$P(\theta_1,\ \theta_2,\ s_3) = P((\theta_1 + \pi),\ (\pi - \theta_2),\ s_3)$. A position-level singularity can be inferred from the relation for θ_2, with $r = 0$, for which singularity requires that $x = 0, y = 0$. It is worth noting that the double solution for θ_1 entails a change of θ_2 also. No such solutions are relevant for the trajectory at hand.

Force Analysis

Following analyses apply the virtual work method throughout. Despite what the figure below may suggest, the effects of the external force and the gravity-induced forces are not taken into consideration in one go.

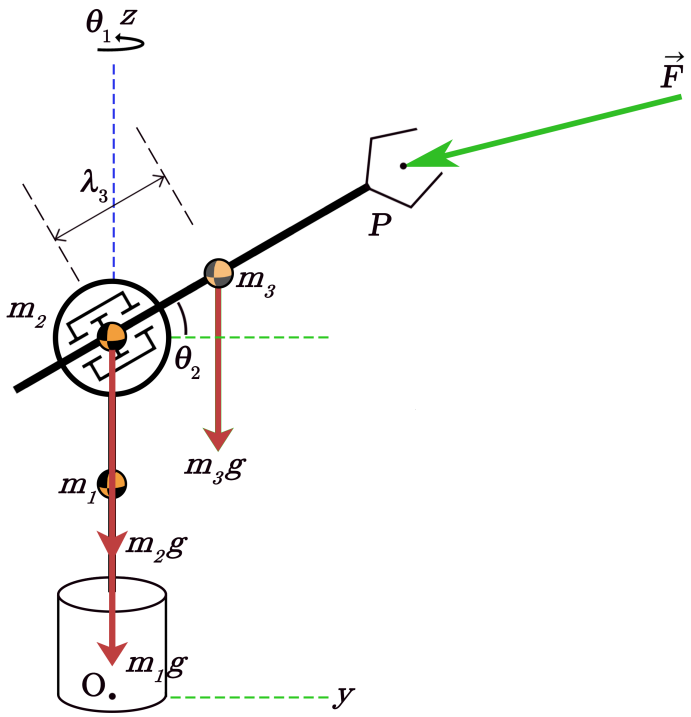

Figure 2.1: Side-view ($y-z$) kinematic diagram of the manipulator ($\theta_1 = 0$).

2.1 Joint Reactions Due to External Force F

An external force, F, is applied at the tip-point of the manipulator, as can be seen in fig. 2.1 above. F is three-dimensional, an is provided as its x-y-z components.

$$\vec{F} = F_x\hat{\imath} + F_y\hat{\jmath} + F_z\hat{k} \tag{2.1}$$

Virtual work method states that the work done by the system over an infinitesimal distance equals the work done on the system over an infinitesimal distance, or in equation

form:

$$F_x\delta x + F_y\delta y + F_z\delta z = \tau_1\delta\theta_1 + \tau_2\delta\theta_2 + f_3\delta s_3 \tag{2.2}$$

Where τ_1, τ_2, and f_3 are reaction torques of revolute joints R_1 and R_2, and the reaction force of the prismatic joint P_1, respectively. Note that x, y and z coordinates were already represented in terms of joint-space parameters in the previous section, in equations 1.2, 1.3, and 1.4. Infinitesimal changes of said equations are as follows:

$$\delta x = \cos\theta_1\cos\theta_2\delta s_3 - \cos\theta_2\sin\theta_1 s_3\delta\theta_1 - \cos\theta_1\sin\theta_2 s_3\delta\theta_2 \tag{2.3}$$

$$\delta y = \sin\theta_1\cos\theta_2\delta s_3 + \cos\theta_1\cos\theta_2 s_3\delta\theta_1 - \sin\theta_1\sin\theta_2 s_3\delta\theta_2 \tag{2.4}$$

$$\delta z = \sin\theta_2\delta s_3 + \cos\theta_2 s_3\delta\theta_2 \tag{2.5}$$

Plugging the above equations into eq. 2.2, and collecting like terms together, we obtain the following relations.

$$\tau_1 = F_x\cos\theta_2\sin\theta_1 s_3 - F_y\cos\theta_1\cos\theta_2 s_3 \tag{2.6}$$

$$\tau_2 = F_x\cos\theta_1\sin\theta_2 s_3 + F_y\sin\theta_1\sin\theta_2 s_3 - F_z\cos\theta_2 s_3 \tag{2.7}$$

$$f_3 = -F_x\cos\theta_1\cos\theta_2 - F_y\sin\theta_1\cos\theta_2 - F_z\sin\theta_2 \tag{2.8}$$

Which can also be represented in matrix form:

$$\begin{bmatrix}\tau_1 & \tau_2 & f_3\end{bmatrix}\begin{bmatrix}\delta\theta_1\\ \delta\theta_2\\ \delta s_3\end{bmatrix} = \begin{bmatrix}F_x & F_y & F_z\end{bmatrix}\begin{bmatrix}\cos\theta_2\sin\theta_1 s_3 & \cos\theta_1\sin\theta_2 s_3 & -\cos\theta_1\cos\theta_2\\ -\cos\theta_1\cos\theta_2 s_3 & \sin\theta_1\sin\theta_2 s_3 & -\sin\theta_1\cos\theta_2\\ 0 & -\cos\theta_2 s_3 & -\sin\theta_2\end{bmatrix}_{3\times3}\begin{bmatrix}\delta\theta_1\\ \delta\theta_2\\ \delta s_3\end{bmatrix}$$

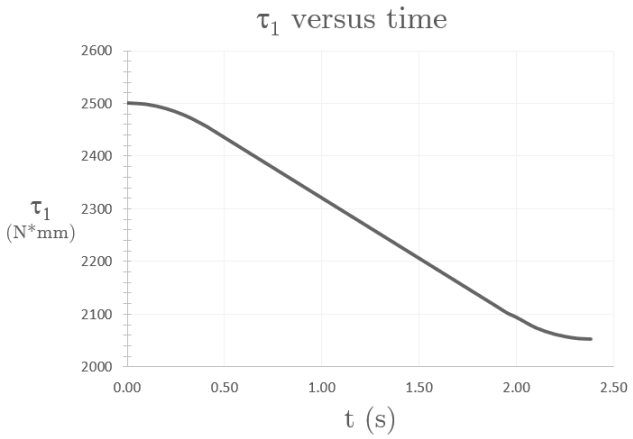

Figure 2.2: Graph of $\tau_1(\mathrm{N}\cdot\mathrm{mm})$ versus time (s) under external load only.

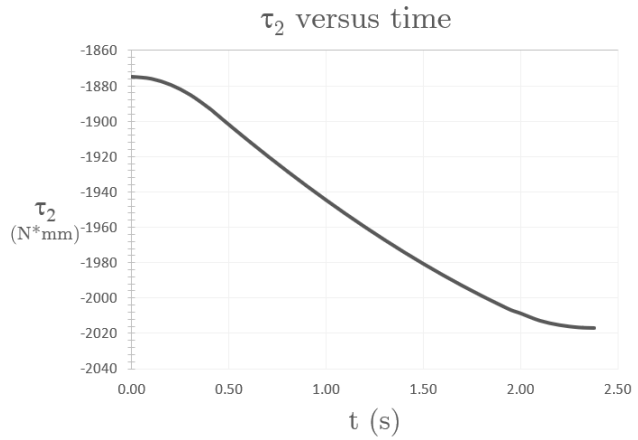

Figure 2.3: Graph of $\tau_2(\mathrm{N}\cdot\mathrm{mm})$ versus time (s) under external load only.

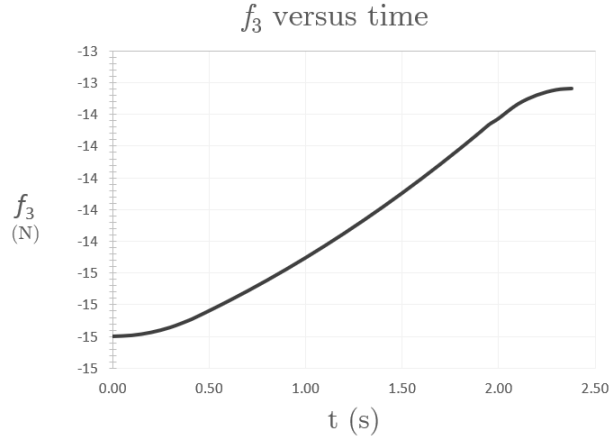

Figure 2.4: Graph of $f_3(\mathrm{N})$ versus time (s) under external load only.

2.2 Joint Reactions Due to Gravitational effects

The resulting forces and torques are merely to counteract the effects of gravity on the manipulator at rest, and do not contribute to the motions.

As can be seen in fig 2.1, of all the weights, the only one *not* coincident with the base of the manipulator is due to m_3, and therefore is the only one necessitating reaction torques/-forces. It should also be stated that for the following to hold, we must assume rigid bodies.

In which case, virtual work principle suggests that:

$$-m_3 g \delta z_3 + \begin{bmatrix} \tau_1 & \tau_2 & f_3 \end{bmatrix} \begin{bmatrix} \delta\theta_1 \\ \delta\theta_2 \\ \delta s_3 \end{bmatrix} = 0 \tag{2.9}$$

where $z_3(\theta_2, s_3)$ is (derivation omitted):

$$z_3 = d_1 + \left(s_3 - \frac{l}{2} \right) \sin\theta_2 \tag{2.10}$$

where $l = s_{3,\,\max}$. Therefore δz_3 is

$$\delta z_3 = \sin\theta_2 \delta s_3 + \left(s_3 - \frac{l}{2} \right) \cos\theta_2 \delta\theta_2 \tag{2.11}$$

Combining equations 2.9 and 2.11,

$$-m_3 g \left[\sin\theta_2 \delta s_3 + \left(s_3 - \frac{l}{2} \right) \cos\theta_2 \delta\theta_2 \right] + \tau_1 \delta\theta_1 + \tau_2 \delta\theta_2 + f_3 \delta s_3 = 0 \tag{2.12}$$

Combining the like terms and canceling them out, we obtain

$$\tau_1 = 0 \tag{2.13}$$

$$\tau_2 = m_3 g \left(s_3 - \frac{l}{2} \right) \cos\theta_2 \tag{2.14}$$

$$f_3 = m_3 g \sin\theta_2 \tag{2.15}$$

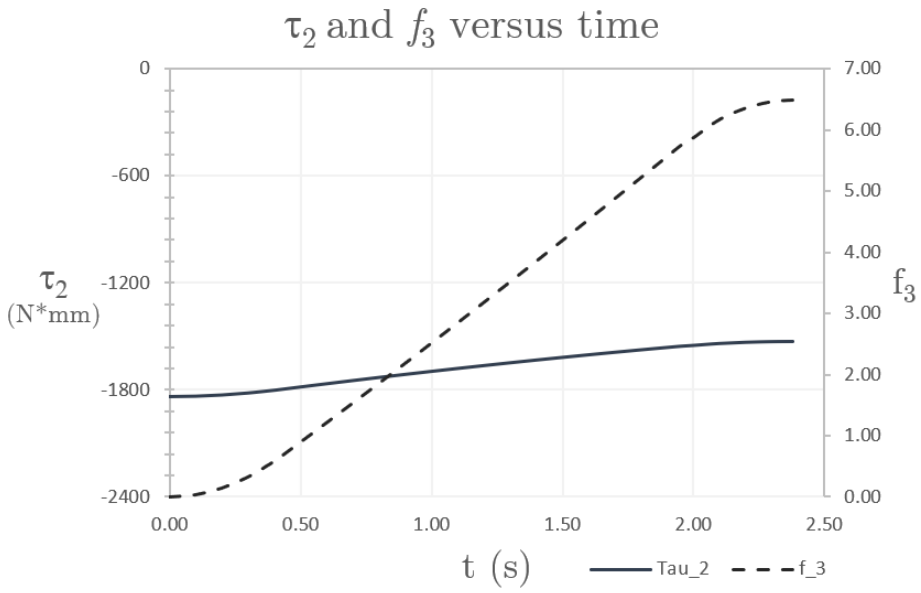

Figure 2.5: Graph of $\tau_2(\mathrm{N}\cdot\mathrm{mm})$ and $f_3(\mathrm{N})$ versus time (s) under gravitational load only.

Tabulated data for the graphs can be found in appendix A.1.

Trajectory & Motion Profile

From project 1, path length is determined to be 31.25 mm.

The path direction is arbitrarily chosen to be orthogonal to the axis $y = -x$, as shown in fig 3.1 below. Destination point and path are mathematically defined in Geogebra.

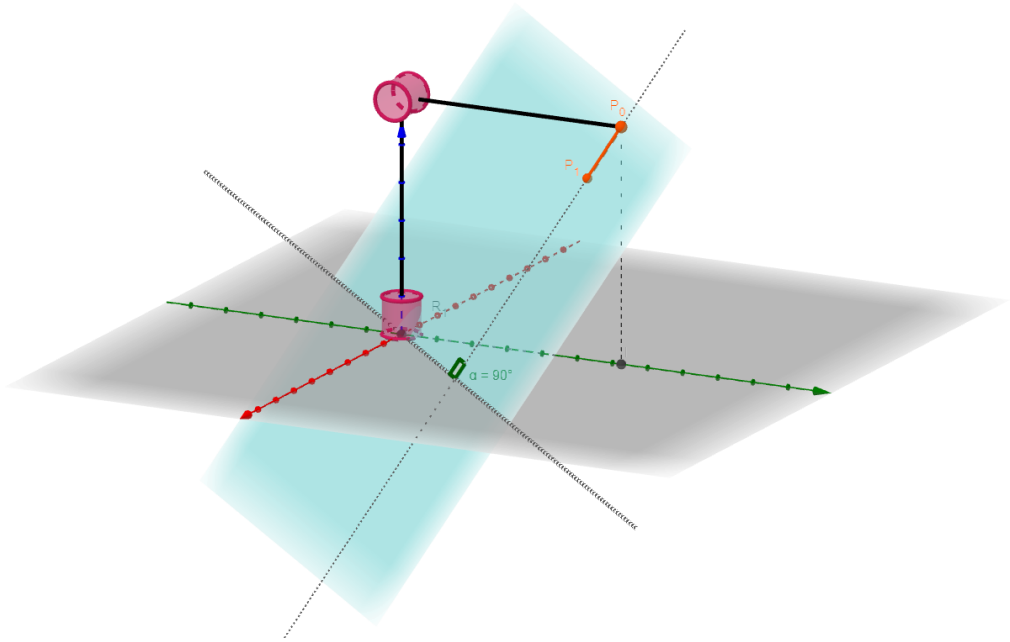

Figure 3.1: Geogebra render of manipulator at home position with the destination point (x axis in green, y axis in red).

The trajectory is sampled at a rate of 10 Hz (per 0.1 seconds) from $t = 0$ and $t = T$. Total travel time T is calculated from the minimum time it takes for the tip point to travel from point P_0 to P_1.

Where P is the displacement vector, T is the total time of travel, subscripts 0 and 1 denote initial and final.

Acceleration during trapezoidal motion profile is as follows:

$$\begin{cases} a_{\max} & 0 \le t \le t_1 \\ 0 & t_1 < t \le t_2 \\ -a_{\max} & t_2 < t \le T \end{cases}$$

Velocity and subsequently displacement can be derived from the above piecewise function via integration or equations of motion.

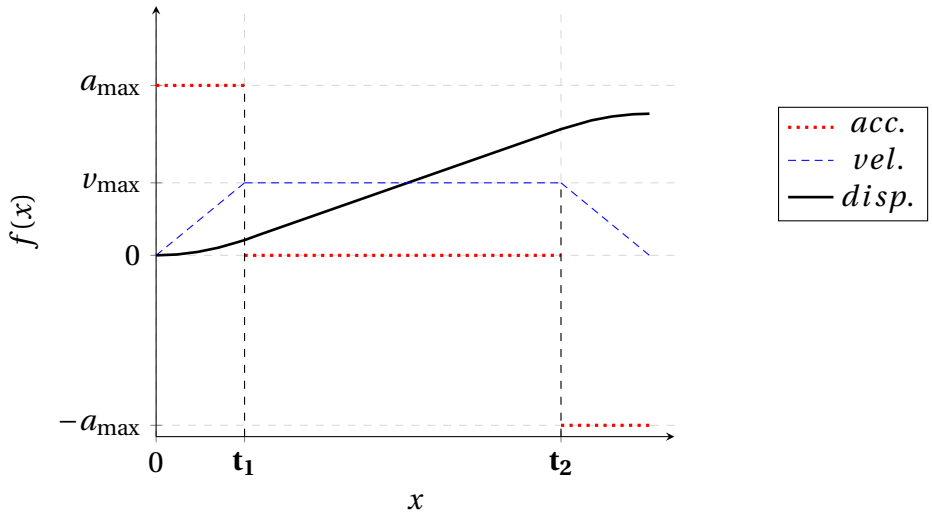

Figure 3.2: Graph of acceleration (mm/s^2), velocity (mm/s) and displacement (mm) versus time (s).

The graph above shows the trapezoidal motion profile, with points of infinite jerk at t_1 and t_2.

Discussion - Conclusion

In the first two parts of the series of projects, position, velocity and acceleration-level forward and inverse kinematics analyses were done. Building on top of the findings of projects #1 and #2, the goal was to conduct quasi-static force analysis on the RRP manipulator. The solutions found can be verified via the old-fashioned statics approach.

References

[1] EMREM, Mert. Forward & Inverse Kinematic Analyses of Serial RRP Manipulator #1. Project Report, 2021. In: İzmir Institute of Technology

[2] EMREM, Mert. Forward & Inverse Kinematic Analyses of Serial RRP Manipulator #2. Project Report, 2021. In: İzmir Institute of Technology

[3] HOHENWARTER, Markus, Michael BORCHERDS , Gabor ANCSIN, Balazs BENCZE and Mathieu BLOSSIER. GeoGebra Classic. computer software. 2021

Appendix

A.1 Data

	Reactions (Gravitational)			**Reactions (External)**		
(s)	(N·mm)	(N·mm)	(N)	(N·mm)	(N·mm)	(N)
t	τ_1	τ_2	f_3	τ_1	τ_2	f_3
0.000	0	-1839	0.000	2500	-1875	-15.00
0.100	0	-1837	0.036	2497	-1876	-14.99
0.200	0	-1830	0.145	2489	-1880	-14.98
0.300	0	-1819	0.326	2476	-1885	-14.94
0.400	0	-1804	0.582	2457	-1893	-14.90
0.427	0	-1799	0.663	2451	-1895	-14.88
0.500	0	-1786	0.895	2434	-1902	-14.84
0.600	0	-1767	1.213	2412	-1911	-14.78
0.700	0	-1750	1.533	2389	-1920	-14.71
0.800	0	-1732	1.857	2366	-1928	-14.65
0.900	0	-1715	2.183	2343	-1937	-14.58
1.000	0	-1698	2.512	2320	-1945	-14.50
1.100	0	-1682	2.843	2297	-1953	-14.43
1.200	0	-1666	3.176	2274	-1960	-14.35
1.300	0	-1650	3.512	2252	-1967	-14.27
1.400	0	-1635	3.849	2229	-1974	-14.18
1.500	0	-1620	4.189	2206	-1981	-14.10
1.600	0	-1605	4.530	2183	-1987	-14.01
1.700	0	-1591	4.872	2160	-1993	-13.91
1.800	0	-1577	5.216	2137	-1999	-13.82
1.900	0	-1564	5.561	2114	-2004	-13.72
1.953	0	-1557	5.744	2102	-2007	-13.66
2.000	0	-1552	5.866	2094	-2009	-13.63
2.100	0	-1542	6.166	2074	-2013	-13.54
2.200	0	-1535	6.353	2062	-2015	-13.48
2.300	0	-1531	6.458	2055	-2017	-13.44
2.380	0	-1530	6.484	2053	-2017	-13.44

A.2 MATLAB Code

```
%%%%%%%%%%%%%%%%%%%     Mert Emrem - 250203015     %%%%%%%%%%%%%%%%%%%%%%
%%%%%%%%%%%%%%%%%%%     ME460 - Project #3         %%%%%%%%%%%%%%%%%%%%%%

clc; clear all

syms theta1(t) theta2(t) s3(t) d1 tau1 tau2 f3 Fx Fy Fz
66

Px = s3(t)*cos(theta2(t))*cos(theta1(t));
Py = s3(t)*cos(theta2(t))*sin(theta1(t));
Pz = d1 + s3(t)*sin(theta2(t));

dx = diff(Px,t); dy = diff(Py,t); dz = diff(Pz,t);


theta1dotx = subs(Fx*dx, [diff(theta2(t), t) diff(s3(t), t)], [0 0]);
theta1doty = subs(Fy*dy, [diff(theta2(t), t) diff(s3(t), t)], [0 0]);
theta1dotz = subs(Fz*dz, [diff(theta2(t), t) diff(s3(t), t)], [0 0]);
theta2dotx = subs(Fx*dx, [diff(theta1(t), t) diff(s3(t), t)], [0 0]);
theta2doty = subs(Fy*dy, [diff(theta1(t), t) diff(s3(t), t)], [0 0]);
theta2dotz = subs(Fz*dz, [diff(theta1(t), t) diff(s3(t), t)], [0 0]);
s3dotx = subs(Fx*dx, [diff(theta1(t), t) diff(theta2(t), t)], [0 0]);
s3doty = subs(Fy*dy, [diff(theta1(t), t) diff(theta2(t), t)], [0 0]);
s3dotz = subs(Fz*dz, [diff(theta1(t), t) diff(theta2(t), t)], [0 0]);


tau1 = -collect(theta1dotx + theta1doty + theta1dotz,diff(theta1(t), t)
    )
tau2 = -collect(theta2dotx + theta2doty + theta2dotz,diff(theta2(t), t)
    )
s3 = -collect((s3dotx + s3doty + s3dotz),diff(s3(t), t))
```